Nonlinear Dyn (2016) 85:1901–1912
DOI 10.1007/s11071-016-2803-4

ORIGINAL PAPER

Non-lane-discipline-based car-following model considering the effect of visual angle

Yongfu Li · Li Zhang · Bo Zhang · Taixiong Zheng · Huizong Feng · Yinguo Li

Received: 12 February 2016 / Accepted: 18 April 2016 / Published online: 28 April 2016

Abstract This study proposes a new car-following (CF) model considering the effect of visual angle under the non-lane-discipline environment. In particular, a car-following model is proposed to capture the impacts from the visual angle of the driver between the following vehicle and the preceding vehicle as well as its change rate on a road without lane discipline. Stability analysis of the proposed CF model is performed using the perturbation method to obtain the stability condition. Numerical experiments analyze three scenarios: start process, stop process, and evolution process for lane-discipline-based FVD model, non-lane-discipline-based CF model with lateral gap, and the proposed model, respectively. Results from numerical experiments illustrate that the proposed CF model that considers the effects of both lateral gap and visual angle has larger stable region compared with FVD model and the NLBCF model. Also, the responsiveness and smoothness of the proposed CF model is improved with respect to the velocity, and acceleration or deceleration profiles.

Keywords Car-following model · Visual angle · Non-lane discipline · Stability analysis

Y. Li (✉) · L. Zhang · T. Zheng · H. Feng · Y. Li
Chongqing Collaborative Innovation Center for Information Communication Technology, College of Automation, Chongqing University of Posts and Telecommunications, Chongqing 400065, China
e-mail: laf1212@163.com

Y. Li
NEXTRANS Center, Purdue University, West Lafayette, IN 47906, USA

B. Zhang
College of Automation, Northwestern Polytechnical University, Xi'an 710072, China

1 Introduction

Traffic problems such as traffic congestion, traffic management, and traffic emissions have received considerable attention recently [1–7]. In order to make effective policies to solve the above-mentioned problems based on the underlying mechanism behind the phenomena of vehicular traffic flow, various traffic flow models have been proposed to capture the behavior of vehicle movement. Traffic flow models can be classified as microscopic or macroscopic models [1–3]. Microscopic models generally use the microscopic variables including velocity, position, and acceleration to capture local interactions between vehicles. Macroscopic models mainly use the collective variables such as the density, volume, and average speed to measure traffic flow properties [8]. This study restricts its focus on the microscopic modeling of vehicular traffic flow.

Microscopic models can be further classified as car-following (CF) models or cellular automation (CA) models. CF models describe the interactions with preceding vehicles in the same lane based on the idea that each driver controls a vehicle under the stimuli from the

preceding vehicle, such as the Gazis–Herman–Rothery (GHR) model [9] and its variations [1–3], Gipps model [10], optimal velocity (OV) model [11] and its variations [12–31], intelligent driver model [32], fuzzy logic model [33], and psycho-physical models [34]. On the other hand, CA models describe the traffic phenomenon using a stochastic discrete approach, such as Rule 184 model [35], Biham–Middleton–Levine (BML) model [36], and Nagel–Schreckenberg (NaSch) model [37] and its variations [2].

The aforementioned traffic flow models can be categorized into lane-discipline-based models, where the models restrict the limitation to the assumption that vehicles follow the lane discipline and move in the middle of the lane. This assumption may not be valid in many developing countries where lanes may not be clearly demarcated on a road though multiple vehicles can travel in parallel [38–42]. Therefore, the lane-discipline-based models may not be readily applied in this scenario. Hence, there is a need to study the impact of lateral gaps on the behavior of the following vehicles. Unlike the lane-discipline-based traffic flow models, several non-lane-discipline-based microscopic traffic flow models have been proposed with focus on the lateral gap of road in recent years [40–42]. To address this scenario, Jin et al. [40] proposed a non-lane-based full velocity difference CF (NLBCF) model to analyze the impact of the unilateral gap on the CF behavior. However, the NLBCF model cannot distinguish the right-side or the left-side lateral gaps. Consequently, Li et al. [41] proposed a generalized model which considers the effects of bilateral gaps of the following vehicle under non-lane-discipline-based environment. In addition, Li et al. [42] further studied the effects of lateral gaps on the energy consumption for electric vehicle (EV) flow. Results from numerical experiments show that the characteristics in terms of lateral distribution of traffic flow may lead to different energy consumption in EV traffic flow.

On the other hand, human factors have been incorporated into CF theory. Andersen et al. [43] discussed the significance of visual angle in CF model theory. Later, Andersen and Sauer [44] proposed the driving by visual angle (DVA) model and suggested that the DVA model was more predictive of driver behavior in matching lead vehicle speed and distance headway. Recently, Zhou [45] incorporated the visual angles' changing rate into the lane-discipline-based FVD model. However, it is not valid for the non-lane-discipline environment. Jin et al. [46] proposed a time to collision equation (TTC)-based general motors (GM) model considering the effect of visual angle information under the non-lane-discipline environment. However, the TTC between the leading vehicle and the following vehicle is difficult to estimate for the driver, while the visual angle and its change is easy to perceive for the driver. Hence, there is a research need to study the effect of human factor, i.e., visual angle and its change, on the vehicular traffic flow-based CF model under the non-lane-discipline environment.

The literature review heretofore illustrates the importance of incorporating the lateral gap and visual angle for modeling traffic flow as well as improving the stability of CF models. Motivated by the scenario with lateral gap and visual angle, the primary objective in this study is to develop a new CF model considering the effects of visual angle and its change rate under the non-lane-discipline environment. The stability of the proposed model is analyzed using the perturbation method to obtain the stability condition. Numerical experiments analyze three scenarios: start process, stop process, and evolution process for lane-discipline-based FVD model, NLBCF model with lateral gap, and the proposed model, respectively. Theoretical and simulation analyses verify that the stability region of the proposed model is improved compared to those of the FVD and NLBCF models under the same condition. Also, results from numerical experiments illustrate that the responsiveness and smoothness of the proposed CF model is improved with respect to the velocity, and acceleration or deceleration profiles.

The rest of this paper is organized as follow: Sect. 2 proposes the new CF model considering the effects of both lateral gap and visual angle. Section 3 performs the stability analysis of proposed model using the perturbation method. Section 4 conducts the numerical experiments and comparisons. The final section concludes this study.

2 Model derivation

In this study, it is assumed that all vehicles travel on a road without lane discipline as shown in Fig. 1. Hence, vehicle may not travel in the middle of the road or follow any lane discipline. The dashed lines in the figure indicate the center lines associated with the various vehicles and are used in the modeling process.

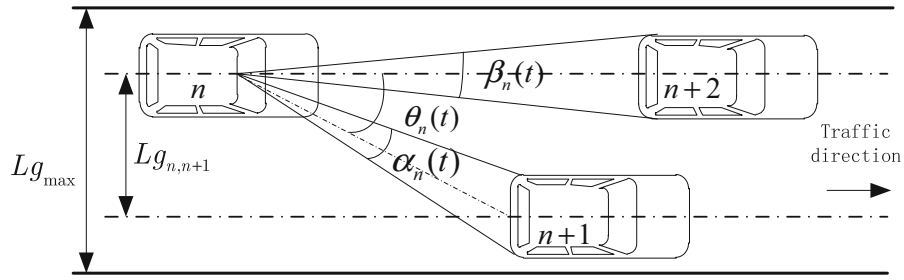

Fig. 1 Car-following model with unilateral gap and visual angle

The leading vehicle (i.e., vehicle $n+2$ in Fig. 1) is traveling in front of the following vehicle (i.e., vehicle n in Fig. 1). The vehicle traveling on the right side of the road (i.e., vehicle $n+1$ in Fig. 1) constitutes the lateral gap with respect to the following vehicle n. Denote $\mathrm{Lg}_{n,n+1}$ as the lateral gap between the following vehicle n and the vehicle traveling laterally $n+1$ and $\mathrm{Lg}_{\max}$ as the maximal lateral gap. Then, the ratio $p_n = \mathrm{Lg}_{n,n+1}/\mathrm{Lg}_{\max} \in [0,1]$ is the parameter to measure the effect of lateral gap. In addition, denote $\theta_n(t)$ as the angle between the center of the leading vehicle $n+2$ to the following vehicle n and the center of the lateral vehicle $n+1$ to the following vehicle n. And $\alpha_n(t)$ is the visual angle between the following vehicle $n+1$ and the lateral vehicle n; $\beta_n(t)$ is the visual angle between the leading vehicle $n+2$ and the following vehicle n. Note that the visual angels defined above both refer to the visual angels that are observed by the driver of the following vehicle n at time t. Hence, we incorporate the effects of visual angle and lateral gap into the CF model and consequently, a new CF model can be formulated as follows:

$$a_n(t) = k\left[V\left(\alpha_n(t), \beta_n(t)\right) - v_n(t)\right] - \kappa \frac{\mathrm{d}G\left(\alpha_n(t), \beta_n(t)\right)}{\mathrm{d}t} \tag{1}$$

where $a_n(t)$ and $v_n(t)$ are the acceleration and velocity of the vehicle n at time t, $k > 0$ and $k \in \mathrm{R}$ and $\kappa \geq 0$ and $\kappa \in \mathrm{R}$ are the sensitivity coefficients. The function $V(\alpha_n(t), \beta_n(t))$ and $G(\alpha_n(t), \beta_n(t))$ are defined as follows:

$$V\left(\alpha_n(t), \beta_n(t)\right) = V\left[(1-p_n)\,\alpha_n(t) + p_n\beta_n(t)\right] \tag{2}$$

$$G\left(\alpha_n(t), \beta_n(t)\right) = (1-p_n)\,\alpha_n(t) + p_n\beta_n(t) \tag{3}$$

And $V(\cdot)$ is the optimal velocity function defined as [12]:

$$V(\Delta x) = V_1 + V_2 \tanh\left[C_1\left(\Delta x - l_c\right) - C_2\right] \tag{4}$$

where V_1, V_2, C_1, C_2 are constant parameters, l_c is the vehicle length, and $\tanh(\cdot)$ is the hyperbolic tangent function. Suppose the width of vehicle is W, and denote $b = \mathrm{Lg}_{n,n+1}$; thus, the visual angles related to the corresponding space headways can be calculated as follows:

$$\begin{aligned} \tan\frac{\beta_n(t)}{2} &= \frac{\frac{W}{2}}{\Delta x_{n,n+2}}, \\ \tan\left(\theta_n(t) + \frac{\alpha_n(t)}{2}\right) &= \frac{b+\frac{W}{2}}{\Delta x_{n,n+1}}, \\ \tan\theta_n(t) &= \frac{b}{\Delta x_{n,n+1}} \end{aligned} \tag{5}$$

where $\Delta x_{n,n+1}(t) = x_{n+1}(t) - x_n(t)$ and $\Delta x_{n,n+2}(t) = x_{n+2}(t) - x_n(t)$ are the space headway between vehicle $n+1$ and vehicle n and vehicle $n+2$ and vehicle n, respectively.

Based on Eq. (5), the visual angles of the driver of the vehicle n can be obtained as follows:

$$\beta_n(t) = 2\arctan\frac{W}{2\Delta x_{n,n+2}} \tag{6}$$

$$\alpha_n(t) = 2\arctan\frac{W\Delta x_{n,n+1}}{2\Delta x_{n,n+1}^2 + b(2b+W)} \tag{7}$$

3 Stability analysis

The stability analysis of the proposed model is performed using the perturbation method under the following assumption:

Assumption 1 Li et al. [41] The initial state of the traffic flow is steady, and all vehicles in the traffic move with the identical safe headway and the optimal velocity.

Based on this assumption, the position solution of the steady traffic flow is:

$$x_n^0(t) = hn + V\left(\alpha_0, \beta_0\right)t \tag{8}$$

where h is the identical safe space headway, α_0, β_0, and $V(\alpha_0, \beta_0)$ are the visual angles and the optimal velocity in uniform traffic flow, respectively.

According to Eqs. (6) and (7), we can obtain

$$\beta_0 = 2\arctan\frac{W}{4h} \tag{9}$$

$$\alpha_0 = 2\arctan\frac{Wh}{2h^2 + b(2b+W)} \tag{10}$$

Adding a small disturbance $y_n(t)$ to the steady-state solution $x_n^0(t)$, i.e.,

$$x_n(t) = x_n^0(t) + y_n(t) \tag{11}$$

Substituting Eq. (11) into Eqs. (9) and (10), the resulting equation can be obtained as:

$$\beta_n(t) = 2\arctan\frac{W}{4h + 2\Delta y_{n,n+2}} \tag{12}$$

$$\alpha_n(t) = 2\arctan\frac{W\left(h + \Delta y_{n,n+1}\right)}{2\left(h + \Delta y_{n,n+1}\right)^2 + b(2b+W)} \tag{13}$$

Substituting Eqs. (11)–(13) into Eq. (1) and linearizing the resulting equation using the Taylor expansion, it deduces

$$\begin{aligned}\ddot{y}_n(t) = k\{&2V'(\alpha_0,\beta_0)[(1-p_n)\\ &\times\left(\arctan\frac{W\left(h+\Delta y_{n,n+1}\right)}{2\left(h+\Delta y_{n,n+1}\right)^2 + b(2b+W)} - \arctan\frac{Wh}{2h^2+b(2b+W)}\right)\\ &+ p_n\left(\arctan\frac{W}{4h+2\Delta y_{n,n+2}} - \arctan\frac{W}{4h}\right)]\\ &- \dot{y}_n(t)\} - \kappa\left[(1-p_n)\frac{\mathrm{d}\alpha_n(t)}{\mathrm{d}t} + p_n\frac{\mathrm{d}\beta_n(t)}{\mathrm{d}t}\right]\end{aligned} \tag{14}$$

Equivalently,

$$\begin{aligned}\ddot{y}_n(t) = k\{&2V'(\alpha_0,\beta_0)\left[(1-p_n)A\Delta y_{n,n+1}\right.\\ &\left.+\ p_nB\Delta y_{n,n+2}\right] - \dot{y}_n(t)\}\\ &-\kappa\left[(1-p_n)C\Delta\dot{y}_{n,n+1} + p_nD\Delta\dot{y}_{n,n+2}\right]\end{aligned} \tag{15}$$

where A, B, C, and D in Eq. (15) are variables defined, respectively, as follows:

$$A = \frac{(2h^2+b(2b+W))W}{(2h^2+b(2b+W))^2+h^2W^2},\quad B = \frac{-2W}{16h^2+W^2},$$

$$C = \frac{2W(2h^2+b(2b+W)) - 8Wh^2}{(2h^2+b(2b+W))^2+W^2h^2},\quad D = \frac{-4W}{16h^2+W^2}$$

Set $y_n(t)$ in the Fourier models, i.e., $y_n(t) = F\exp(\mathrm{i}\alpha n + zt)$; substituting it in Eq. (15), we have

$$\begin{aligned}z^2 = k&\left\{2V'\left[(1-p_n)A\left(\mathrm{e}^{\mathrm{i}\alpha}-1\right) + p_nB\left(\mathrm{e}^{2\mathrm{i}\alpha}-1\right)\right] - z\right\}\\ &-\kappa\left[(1-p_n)Cz\left(\mathrm{e}^{\mathrm{i}\alpha}-1\right) + p_nDz\left(\mathrm{e}^{2\mathrm{i}\alpha}-1\right)\right]\end{aligned} \tag{16}$$

Let $z = z_1(\mathrm{i}\alpha) + z_2(\mathrm{i}\alpha)^2 + \cdots$ and expand it to the second term of $(\mathrm{i}\alpha)$ in Eq. (16), and we obtain

$$\begin{aligned}z_1^2(\mathrm{i}\alpha)^2 = k\Big\{&2V'\left[(1-p_n)A\left((\mathrm{i}\alpha) + \frac{1}{2}(\mathrm{i}\alpha)^2\right)\right.\\ &\left.+\ p_nB\left((2\mathrm{i}\alpha) + \frac{1}{2}(2\mathrm{i}\alpha)^2\right)\right]\\ &-\ z_1(\mathrm{i}\alpha) - z_2(\mathrm{i}\alpha)^2\Big\}\\ &-\kappa\Big[(1-p_n)C\left(z_1(\mathrm{i}\alpha)\right.\\ &\left.+\ z_2(\mathrm{i}\alpha)^2\right)\left((\mathrm{i}\alpha) + \frac{1}{2}(\mathrm{i}\alpha)^2\right)\\ &+ p_nD\left(z_1(\mathrm{i}\alpha) + z_2(\mathrm{i}\alpha)^2\right)\\ &\times\left((2\mathrm{i}\alpha) + \frac{1}{2}(2\mathrm{i}\alpha)^2\right)\Big]\end{aligned} \tag{17}$$

Therefore,

$$\begin{cases}0 = k\left\{2V'\left[(1-p_n)A + 2p_nB\right] - z_1\right\}\\ z_1^2 = k\left\{2V'\left[\frac{(1-p_n)A}{2} + 2p_nB\right] - z_2\right\}\\ \quad -\kappa\left[(1-p_n)Cz_1 + 2p_nDz_1\right]\end{cases} \tag{18}$$

Consequently,

$$\begin{cases}z_1 = 2V'\left[(1-p_n)A + 2p_nB\right]\\ z_2 = 2V'\left[\frac{(1-p_n)A}{2} + 2p_nB\right]\\ \quad -\frac{z_1^2+\kappa[(1-p_n)C+2P_nD]z_1}{a}\end{cases} \tag{19}$$

Let $z_1 > 0$ and $z_2 > 0$, and we can obtain the stability condition as follows:

$$\begin{cases}p_n < \frac{A}{A-4B} \quad \text{where } A > 0,\ B < 0\\ a > \frac{4V'[(1-p_n)A+2p_nB]^2+2\kappa[(1-p_n)C+2pD][(1-p_n)A+2p_nB]}{(1-p_n)A+4p_nB}\end{cases} \tag{20}$$

Finally, the neutral curve can be presented as:

$$\tau = \frac{(1-p_n)A + 4p_nB}{4V'[(1-p_n)A+2p_nB]^2+2\kappa[(1-p_n)C+2p_nD][(1-p_n)A+2p_nB]} \tag{21}$$

4 Numerical experiments

4.1 Steady performance

Based on the foregoing analysis, this section presents numerical experiments to verify the steady performance of the proposed model in terms of the stability region. The initial conditions are set as follows:

$$h = 2,\ b = 1,\ W = 2 \tag{22}$$

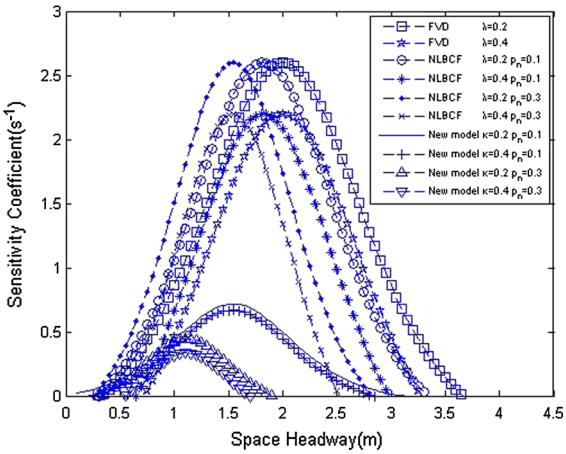

Fig. 2 Critical curves of FVD model, NLBCF model, and the proposed model in the space headway–sensitivity coefficient diagram with different coefficients

Table 1 Values of parameters in the CF models

Parameter	Value	Unit
k	0.85	s^{-1}
λ	0.3	s^{-1}
v_{max}	2.0	m/s
V_1	6.75	m/s
V_2	7.91	m/s
C_1	0.13	m^{-1}
C_2	1.57	–
l_c	5.0	m
p_n	0.3	–

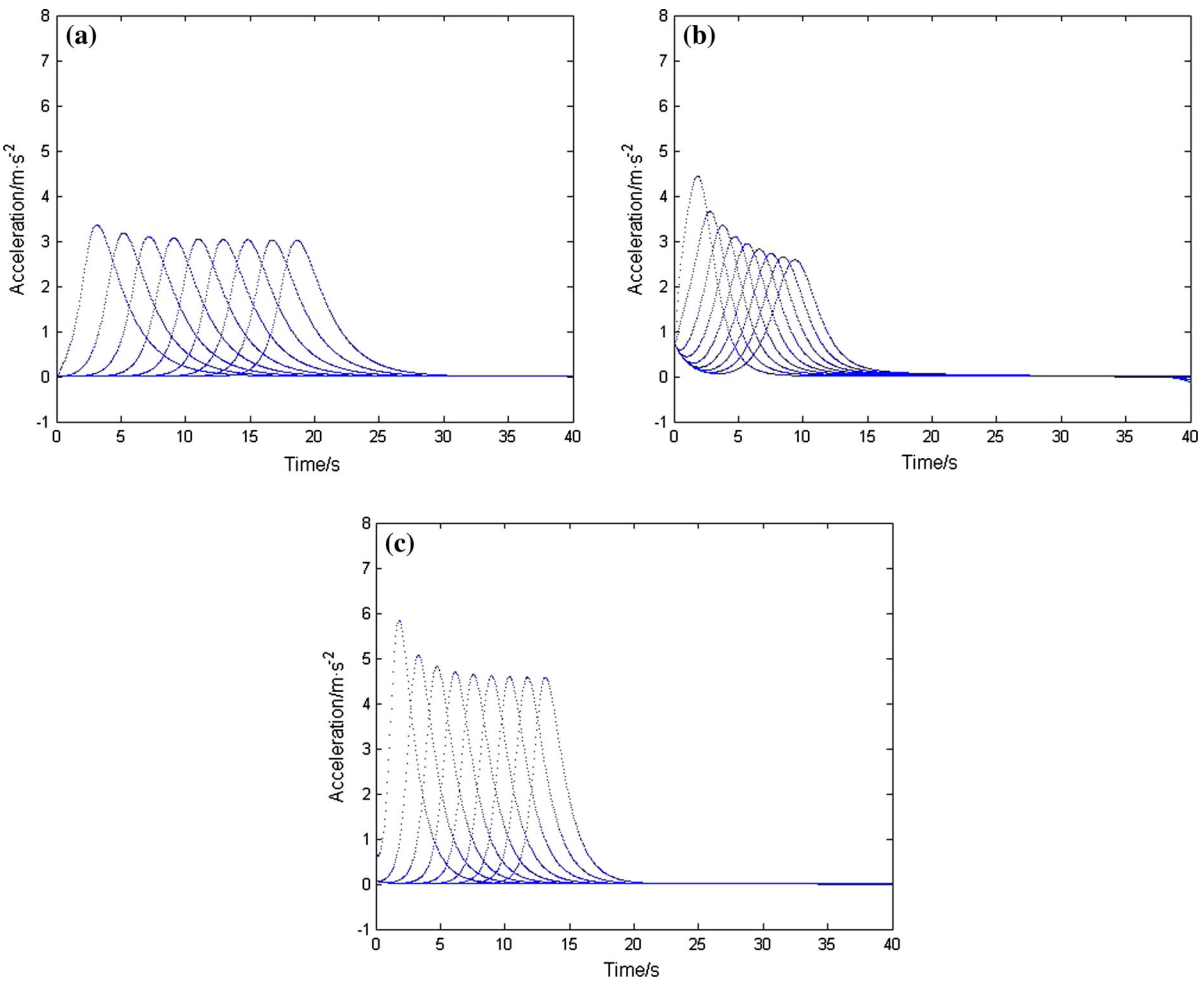

Fig. 3 Acceleration profile of traffic stream starting from a green traffic signal: **a** FVD model; **b** NLBCF model; **c** the proposed model ($\kappa = 0.3\,\mathrm{m/s^{-2}\,degree^{-1}}$)

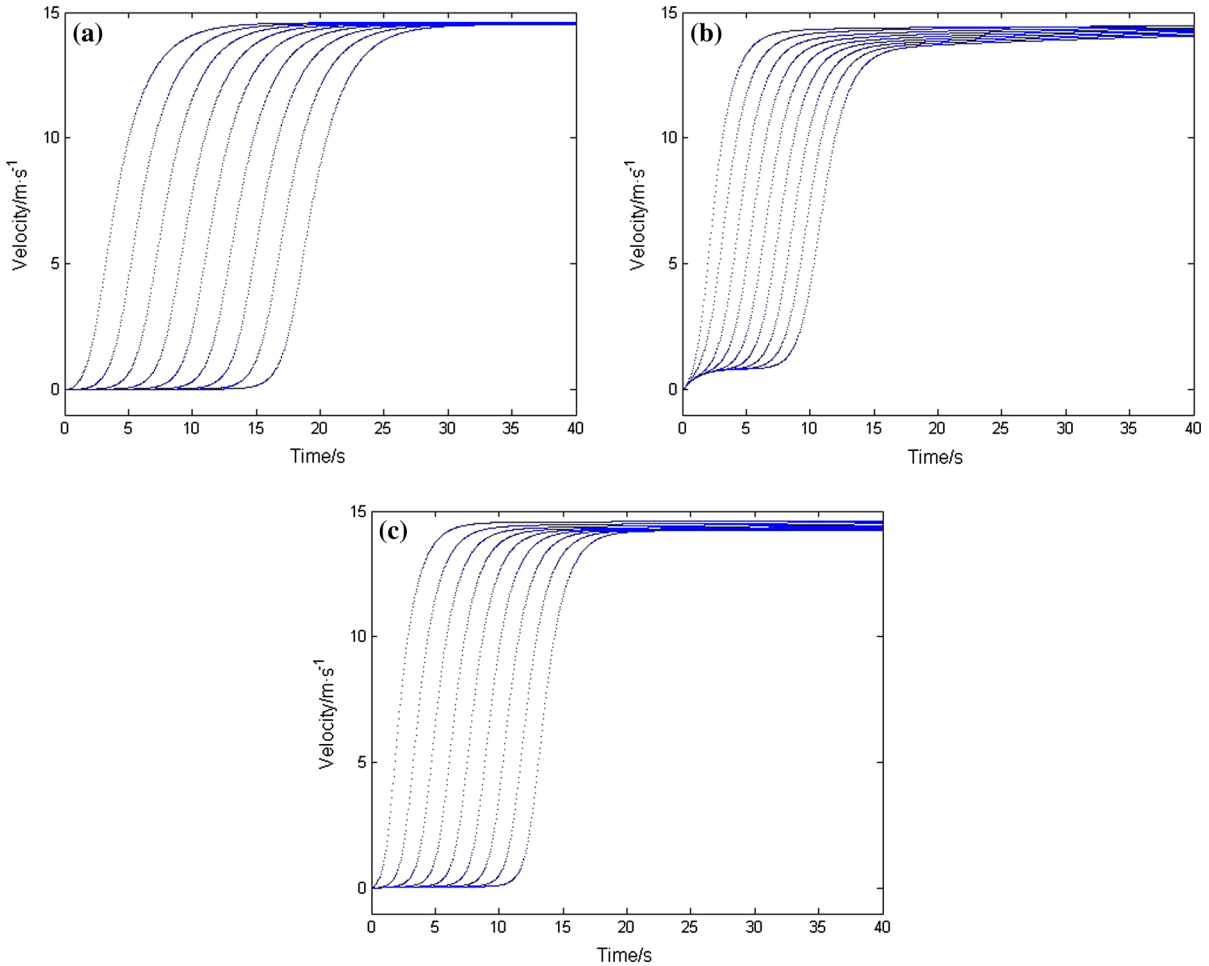

Fig. 4 Velocity profile of traffic stream starting from a green traffic signal: **a** FVD model; **b** NLBCF model; **c** the proposed model ($\kappa = 0.3\,\mathrm{m/s^{-2}\,degree^{-1}}$)

According to Eq. (22), we can obtain $A = \frac{3}{20}$, $B = -\frac{1}{17}$, $C = -\frac{1}{10}$, $D = -\frac{2}{17}$. Figure 2 shows the critical curves among sensitivity coefficient λ in FVD model or NLBCF model, κ in the proposed model and the space headway. In Fig. 2, the space formed by the sensitivity coefficient and the space headway is divided into two regions (stable region and unstable region) by the critical curve. Specifically, the region over each critical curve is the stable region in which the traffic flow is stable; the remainder is the unstable region in which density waves emerge.

Based on Fig. 2, by comparing the results under no lateral gap, lateral gap, and both lateral gap and visual angles conditions, the main findings are summarized as follows: (1) The stable region of traffic flow will be enlarged with the increase in coefficients in the case of the same value of parameter p_n. This pattern is similar for the FVD model, NLBCF model, and the proposed model; (2) comparisons between FVD model and NLBCF model show that the critical curves will be shifted left from the initial state with the increase in parameter p_n in the case of the same value of coefficient, and the stable region is nearly unchanged; (3) comparisons between FVD model and the proposed model show that when the effects of both the lateral gap and visual angle are taken into consideration, the stability region of proposed model is enlarged significantly; (4) comparisons between NLBCF model and the proposed model show that when the effect of visual angles is considered under the non-lane-discipline environment, the stability region of proposed model is also enlarged; (5) the steady performance of the uniform

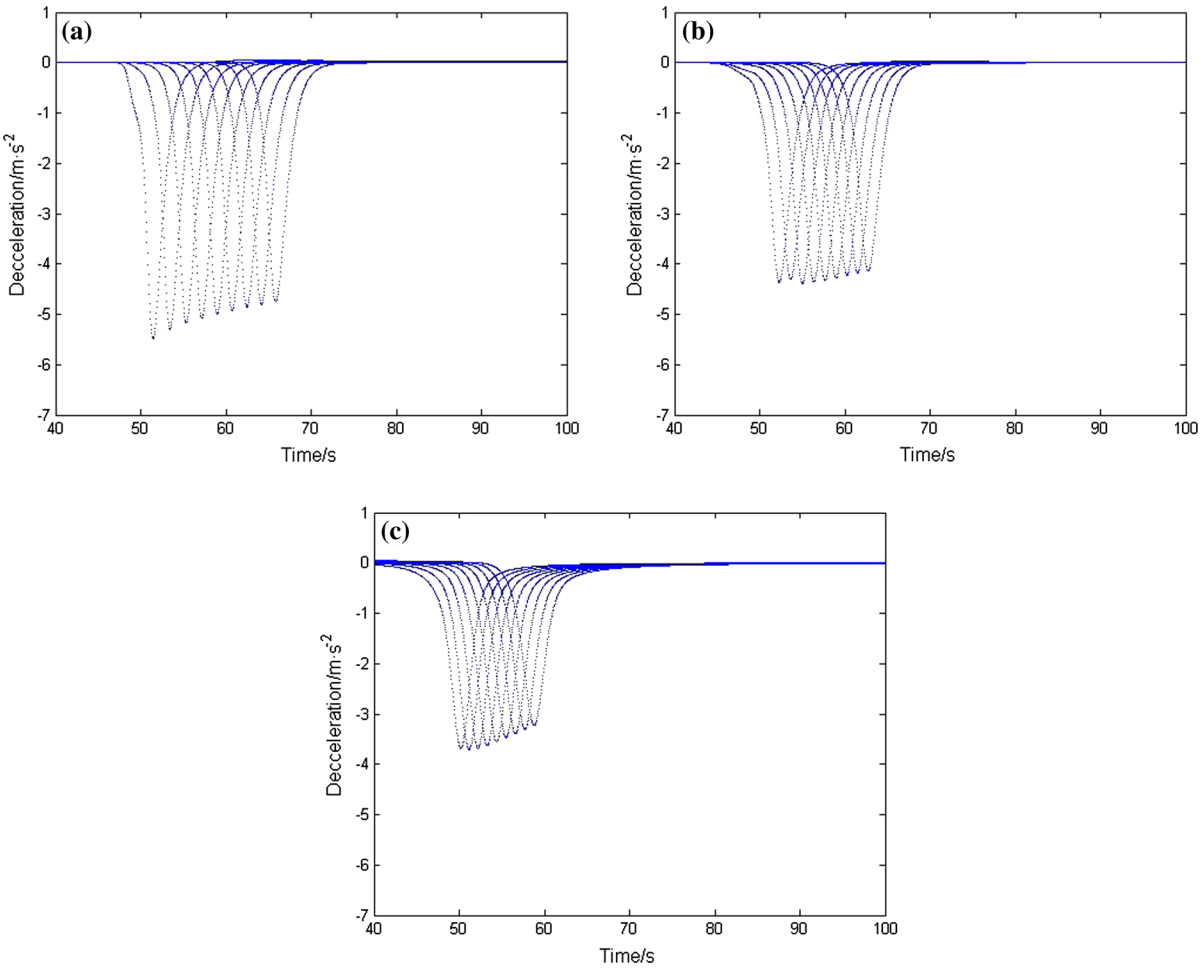

Fig. 5 Deceleration profile of traffic stream stopping at a red traffic signal: **a** FVD model; **b** NLBCF model; **c** the proposed model ($\kappa = 180\,\mathrm{m/s^{-2}\,degree^{-1}}$)

traffic flow will be improved by considering the effects of both lateral gap and visual angle compared with FVD model and NLBCF model under the same condition.

4.2 Dynamic performance

This section provides numerical experiments to verify the dynamic performance of the proposed model. In order to illustrate the dynamic performance of FVD model without lateral gap and visual angle, NLBCF model only with lateral gap, and the proposed model with both lateral gap and visual angle, we compare simulation results of the three models under the start, stop, and evolution processes, respectively. The initial condition is as follows. Nine vehicles are distributed in a road with the equal space headway of 7.4 m. And the ninth vehicle is the leading one. The values of parameters used in the numerical experiment are shown in Table 1. Other conditions are set the same as in [40–42,45].

4.2.1 Start process

The start process is set up as follows. Initially, the traffic signal is red, and all vehicles are waiting behind the signal with the uniform space headway. At time $t = 0\,\mathrm{s}$, the signal changes to green and the vehicles start to move. The leading vehicle starts to accelerate until it reaches the optimal velocity. The other vehicles follow the leading vehicle to accelerate. Eventually, all vehicles travel at the same optimal velocity. For com-

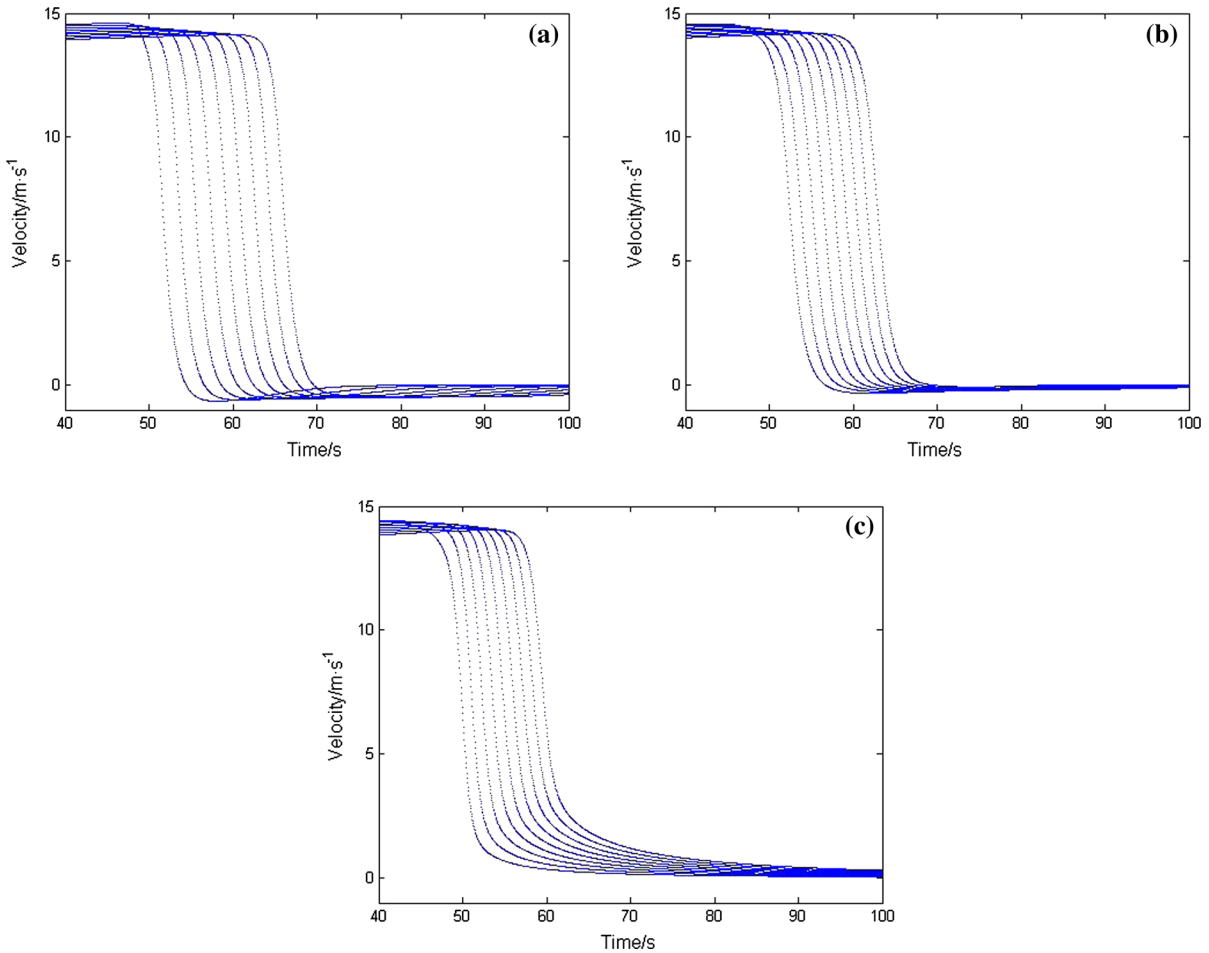

Fig. 6 Velocity profile of traffic stream stopping at a red traffic signal: **a** FVD model; **b** NLBCF model; **c** the proposed model ($\kappa = 180\,\mathrm{m/s^{-2}\,degree^{-1}}$)

parison, the acceleration and velocity profiles of FVD model, NLBCF model, and the proposed model are illustrated in Figs. 3 and 4, respectively.

Figure 3 demonstrates that the magnitude of acceleration for FVD model is the least, followed by NLBCF model, then the proposed model. That is because the FVD model is based on the lane discipline, while the NLBCF model and the proposed model are based on non-lane discipline. Therefore, drivers can accelerate aggressively. In addition, the following vehicles in FVD model can follow the consensus state of the leading vehicles well, but it needs a long time to finish the acceleration phase; the vehicles in NLBCF model can finish the acceleration phase quickly, but the following vehicles cannot follow the consensus state of the leading vehicles well, especially at the beginning stage. Vehicles in the proposed model considering the effect of both lateral gap and visual angle can keep the consensus state and finish acceleration phase in a shorter time. Figure 4 shows that the FVD model without lateral gap and visual angle possesses a delay time at the acceleration phase. And the NLBCF model with lateral gap but without visual angle is the most responsive; however, vehicles in the NLBCF model possess an unrealistic initial velocity at the beginning of acceleration. The proposed model with both lateral gap and visual angle has a shorter delay time compared with the FVD model. Meanwhile, the proposed model also has a better realistic initial velocity compared with the NLBCF model. Hence, the dynamic performance in the start process of the proposed model is best with respect to the smoothness and responsiveness.

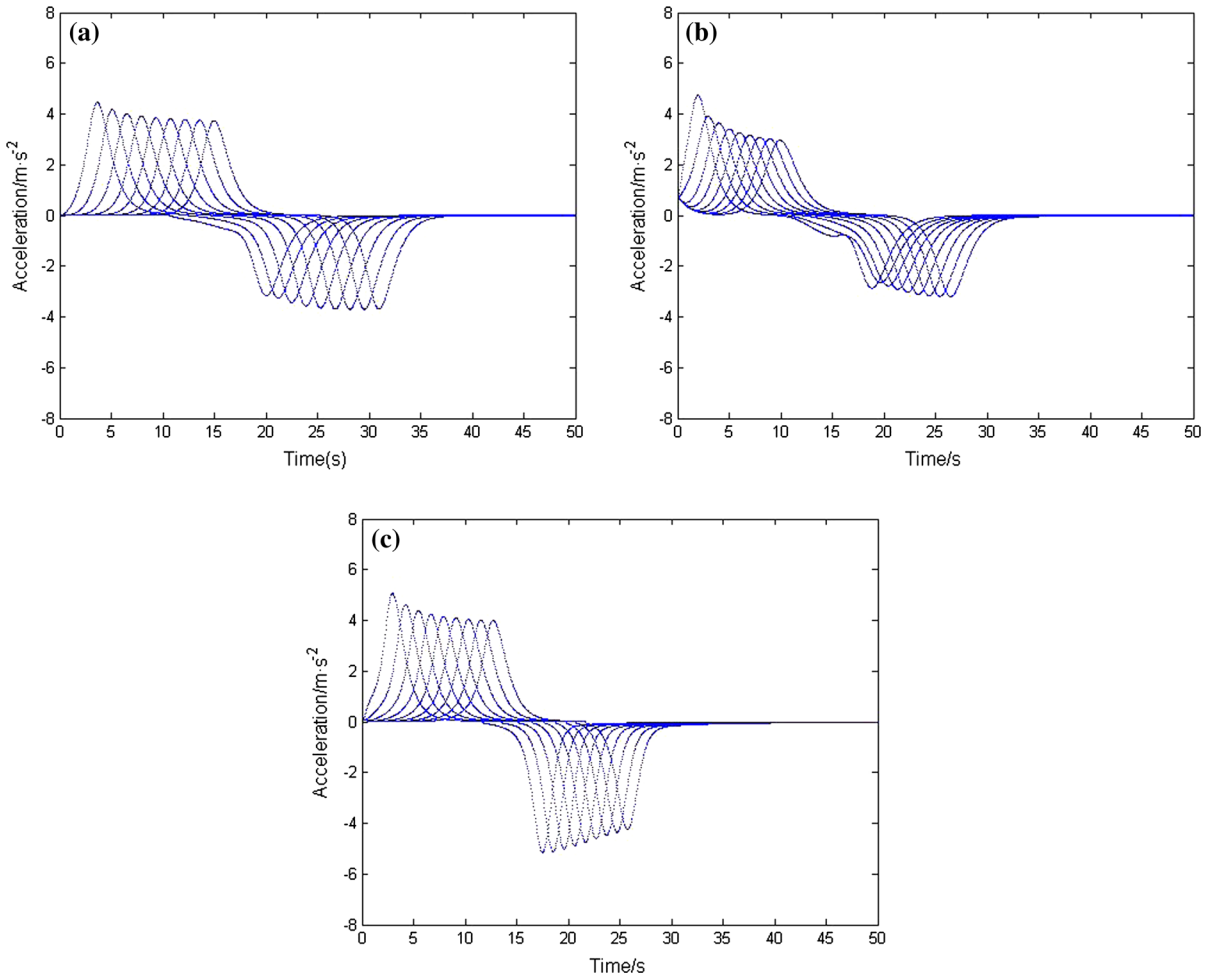

Fig. 7 Acceleration profile of traffic stream evolution: **a** FVD model; **b** NLBCF model; **c** the proposed model ($\kappa = 180\,\mathrm{m/s^{-2}\,degree^{-1}}$)

4.2.2 Stop process

The stop process is set up as follows. Initially, the traffic signal is green and all vehicles are traveling at the same constant velocity. At time $t = 0$ s, the signal changes to red and vehicles begin to slow down. The leading vehicle begins to decelerate until it reaches a full stop. The other vehicles follow the leading vehicle to decelerate. Finally, all vehicles fully stop behind the signal. For comparison, the deceleration and velocity profiles of FVD model, NLBCF model, and the proposed model are illustrated in Figs. 5 and 6, respectively.

Figure 5 demonstrates that the magnitude of deceleration for the proposed model is the least, followed by NLBCF model, then FVD model, and the profiles of the proposed model are smoothest. It implies that the best comfortable driving pattern can be provided by the proposed model compared with the FVD model and NLBCF model at the stop process. Figure 6 also illustrates that the proposed model is smoother than the FVD model and NLBCF model. In addition, both the FVD model and NLBCF model have the unrealistic negative velocity at the end of the stop process. However, the proposed model avoids this deficiency by incorporating the effect of visual angle. Therefore, the dynamic performance in the stop process of the proposed model is best compared with the FVD model and NLBCF model.

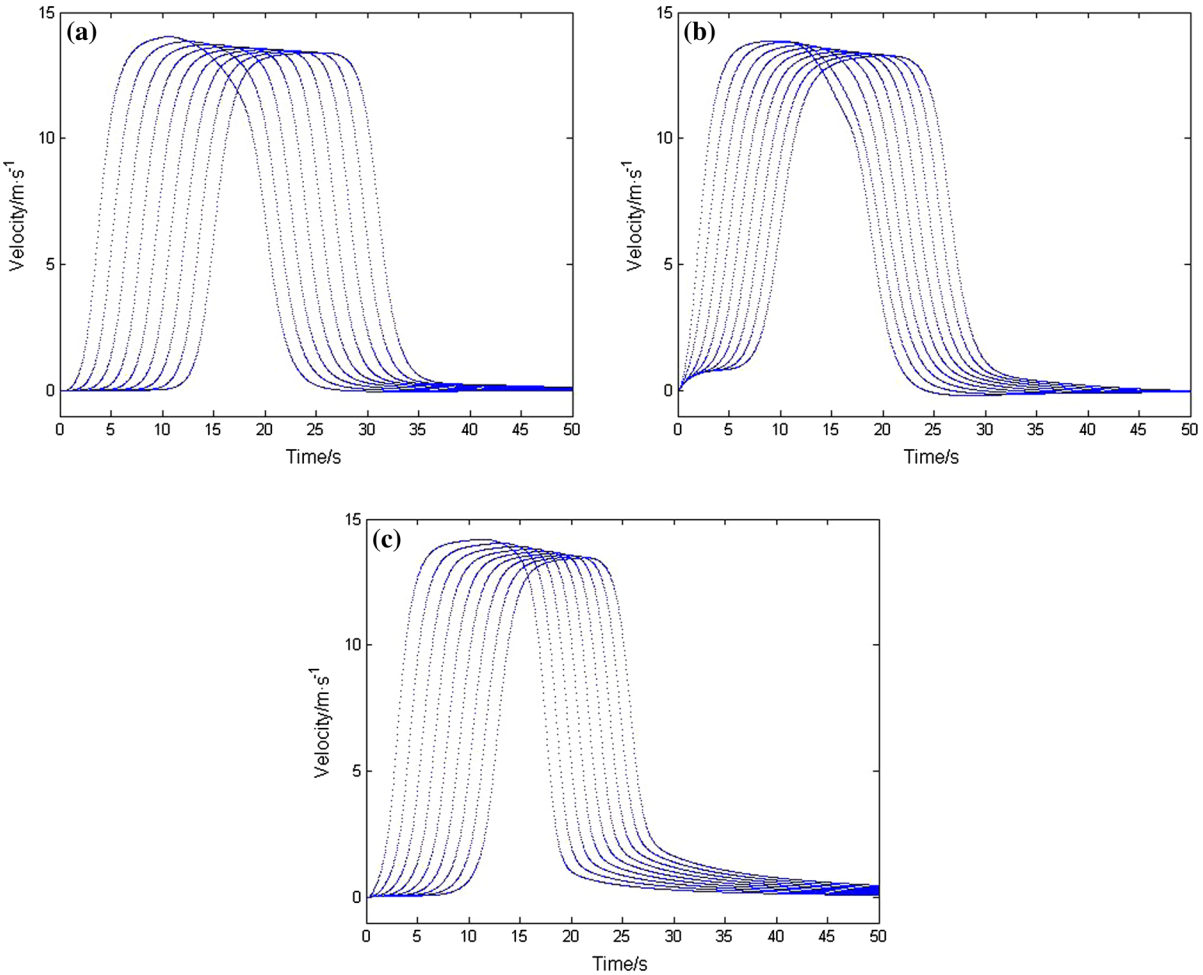

Fig. 8 Velocity profile of traffic stream evolution: **a** FVD model; **b** NLBCF model; **c** the proposed model ($\kappa = 180\,\mathrm{m/s^{-2}\,degree^{-1}}$)

4.2.3 Evolution process

The evolution process is discussed by combining the start and stop processes. The leading vehicle first starts to move from the zero velocity and then decelerates to a full stop. The other vehicles follow the leading vehicle according to FVD model, NLBCF model, and the proposed model, respectively. For comparison, Figs. 7 and 8 show the acceleration and the velocity profiles.

Figure 7 shows that vehicles in the FVD model and NLBCF model start to accelerate or decelerate one by one with a transition period. Vehicles in the proposed model, however, accelerate or decelerate more quickly. In addition, the distribution of the acceleration profiles in the proposed model is the most regular for both the leading vehicle and the following vehicles. It implies that the distribution of the acceleration profiles of the proposed model is the most symmetrical between the start and stop processes. Figure 8 demonstrates that the proposed model is most responsive, followed by the NLBCF model, and then the FVD model, which is consistent with the observations in the start and stop processes. It also shows that vehicles in the proposed model can move smoother than the FVD model and NLBCF model and the unrealistic traffic phenomenon does not occur at either the start process or the stop process.

Based on the theoretical analyses and numerical experiments, the comparisons demonstrate the steady performance in terms of the stable region and the dynamic performance in terms of the responsiveness and smoothness of the proposed model are improved

by considering the effects of both lateral gap and visual angle, compared with the lane-discipline-based FVD model and the non-lane-discipline-based NLBCF model with lateral gap.

5 Conclusions

Considering the effects of both lateral gap and visual angel, a new CF model is proposed in this study. Theoretical analysis proves that the proposed model is more generalized than the lane-discipline-based FVD model and the NLBCF model. Compared with the FVD model and NLBCF model, the steady performance in terms of the stability region of the proposed model is best through the stability analysis using the perturbation method. In addition, numerical experiments are performed to illustrate the effects of lateral gap and visual angel on the responsiveness and smoothness with respect to the acceleration and velocity profiles in the start, stop, and evolution processes.

Simulation results show that the steady and dynamic performance of the proposed model is better than those of the FVD model and NLBCF model in terms of the stability and responsiveness as well as smoothness, respectively. The findings of this study provide insights that we can capture and characterize the traffic phenomenon more realistically by incorporating the human factors.

Acknowledgments This work is jointly supported by the National Natural Science Foundation of China under Grant 61304197, the Scientific and Technological Talents of Chongqing under Grant cstc2014kjrc-qnrc30002, the Key Project of Application and Development of Chongqing under Grant No. cstc2014yykfB40001, Wenfeng Talents of CQUPT, 151 Science and Technology Major Project of Chongqing-General Design and Innovative Capability of Full Information based Traffic Guidance and Control System under Grant No. cstc2013jcsfzdzxqqX0003, the Natural Science Funds of Chongqing under Grant No. cstc2014jcyjA60003, and the Doctoral Start-up Funds of CQUPT under Grant No. A2012-26.

References

1. Wilson, R., Ward, J.: Car-following models: fifty years of linear stability analysis-a mathematical perspective. Transp. Plan. Technol. **34**(1), 3–18 (2011)
2. Li, Y., Sun, D.: Microscopic car-following model for the traffic flow: the state of the art. J. Control Theory Appl. **10**(2), 133–143 (2012)
3. Saifuzzaman, M., Zheng, Z.: Incorporating human-factors in car-following models: a review of recent developments and research needs. Transp. Res. C **48**, 379–403 (2014)
4. Li, Y., Yang, B., Zheng, T., Li, Y., Cui, M., Peeta, S.: Extended-state-observer-based double loop integral sliding mode control of electronic throttle valve. IEEE Trans. Intell. Transp. Syst. **16**, 2501–2510 (2015)
5. Li, Y., Li, K., Zheng, T., Hu, X., Feng, H., Li, Y.: Evaluating the performance of vehicular platoon control under different network topologies of initial states. Phys. A **450**, 359–368 (2016)
6. Ouyang, M., Zhao, L., Hong, L., Pan, Z.: Comparisons of complex network based models and real train flow model to analyze Chinese railway vulnerability. Reliab. Eng. Syst. Saf. **123**, 38–46 (2014)
7. Hong, L., Ouyang, M., Peeta, S., He, X., Yan, Y.: Vulnerability assessment and mitigation for the Chinese railway system under floods. Reliab. Eng. Syst. Saf. **137**, 58–68 (2015)
8. Li, Y., Zhang, L., Zheng, T., Li, Y.: Lattice hydrodynamic model based delay feedback control of vehicular traffic flow considering the effects of density change rate difference. Commun. Nonlinear Sci. Numer. Simul. **29**(1–3), 224–232 (2015)
9. Gazis, D., Herman, R., Rothery, R.: Nonlinear follow the leader models of traffic flow. Oper. Res. **9**(4), 545–567 (1961)
10. Gipps, P.: A behavioral car-following model for computer simulation. Transp. Res. B **15**(2), 105–111 (1981)
11. Bando, M., Hasebe, K., Nakayama, A., Shibata, A., Sugiyama, Y.: Dynamics model of traffic congestion and numerical simulation. Phys. Rev. E **51**(2), 1035–1042 (1995)
12. Helbing, D., Tilch, B.: Generalized force model of traffic dynamics. Phys. Rev. E **58**, 133–138 (1998)
13. Jiang, R., Wu, Q., Zhu, Z.: Full velocity difference model for a car-following theory. Phys. Rev. E **64**, 017101–017105 (2001)
14. Sun, D., Li, Y., Tian, C.: Car-following model based on the information of multiple ahead and velocity difference. Syst. Eng. Theory Pract. **30**(7), 1326–1332 (2010)
15. Zhao, X., Gao, Z.: A new car-following model: full velocity and acceleration difference model. Eur. Phys. J. B **47**(1), 145–150 (2005)
16. Wang, T., Gao, Z., Zhao, X.: Multiple velocity difference model and its stability analysis. Acta Phys. Sin. **55**, 634–640 (2006)
17. Li, Y., Sun, D., Liu, W., Zhang, M., Zhao, M., Liao, X., Tang, L.: Modeling and simulation for microscopic traffic flow based on multiple headway, velocity and acceleration difference. Nonlinear Dyn. **66**(1), 15–28 (2011)
18. Tang, T., Wang, Y., Yang, X., Wu, Y.: A new car-following model accounting for varying road condition. Nonlinear Dyn. **70**(2), 1397–1405 (2012)
19. Tang, T., Shi, W., Shang, H., Wang, Y.: A new car-following model with consideration of inter-vehicle communication. Nonlinear Dyn. **76**, 2017–2023 (2014)
20. Tang, T., Wang, Y., Yang, X., Huang, H.: A multilane traffic flow model accounting for lane width, lane-changing and the number of lanes. Netw. Spat. Econ. **14**, 465–483 (2014)
21. Tang, T., He, J., Yang, S., Shang, H.: A car-following model accounting for the driver's attribution. Phys. A **413**, 583–591 (2014)

22. Tang, T., Chen, L., Yang, S., Shang, H.: An extended car-following model with consideration of the electric vehicle's driving range. Phys. A **430**, 148–155 (2015)
23. Yu, S., Shi, Z.: Analysis of car-following behaviors considering the green signal countdown device. Nonlinear Dyn. **82**(1–2), 731–740 (2015)
24. Delpiano, R., Laval, J., Coeymans, J., Herrera, J.: The kinematic wave model with finite decelerations: a social force car-following model approximation. Transp. Res. B **71**, 182–193 (2015)
25. Tang, T., Shi, W., Shang, H., Wang, Y.: An extended car-following model with consideration of the reliability of inter-vehicle communication. Measurement **58**, 286–293 (2014)
26. Yu, S., Shi, Z.: An extended car-following model considering relative velocity fluctuation. Commun. Nonlinear Sci. Numer. Simul. **36**, 319–326 (2016)
27. Yu, S., Shi, Z.: Dynamics of connected cruise control systems considering velocity changes with memory feedback. Measurement **64**, 34–48 (2015)
28. Yu, S., Shi, Z.: An extended car-following model at signalized intersections. Phys. A **407**, 152–159 (2014)
29. Ge, J., Orosz, G.: Dynamics of connected vehicle systems with delayed acceleration feedback. Transp. Res. C **46**, 46–64 (2014)
30. Yu, S., Shi, Z.: The effects of vehicular gap changes with memory on traffic flow in cooperative adaptive cruise control strategy. Phys. A **428**, 206–223 (2015)
31. Yu, S., Liu, Q., Li, X.: Full velocity difference and acceleration model for a car-following theory. Commun. Nonlinear Sci. Numer. Simul. **18**, 1229–1234 (2013)
32. Treiber, M., Hennecke, A., Helbing, D.: Congested traffic states in empirical observations and microscopic simulations. Phys. Rev. E **62**, 1805–1824 (2000)
33. Kikuchi, C., Chakroborty, P.: Car following model based on a fuzzy inference system. Transp. Res. Rec. **1365**, 82–91 (1992)
34. Michaels, R.: Perceptual factors in car following. In: Proceedings of the Second International Symposium on the Theory of Road Traffic Flow, pp. 44–59. London (1963)
35. Wolfram, O.: Theory and application of cellular automata. In: Proceedings of World Scientific, Singapore (1986)
36. Biham, O., Middleton, A., Levine, D.: Self-organization and a dynamical transition in traffic-flow models. Phys. Rev. A **46**(10), 6124–6127 (1992)
37. Nagel, K., Schreckenberg, M.: A cellular automaton model for freeway traffic. J. Phys. **2**(12), 2221–2229 (1992)
38. Chandra, S., Kumar, U.: Effect of lane width on capacity under mixed traffic conditions in India. J. Transp. Eng. **129**(2), 155–160 (2003)
39. Gunay, B.: Car following theory with lateral discomfort. Transp. Res. B **41**(7), 722–735 (2007)
40. Jin, S., Wang, D., Tao, P., Li, P.: Non-lane-based full velocity difference car following model. Phys. A **389**(21), 4654–4662 (2010)
41. Li, Y., Zhang, L., Peeta, S., Pan, H., Zheng, T., Li, Y., He, X.: Non-lane-discipline-based car-following model considering the effects of two-sided lateral gaps. Nonlinear Dyn. **80**(1–2), 227–238 (2015)
42. Li, Y., Zhang, L., Zheng, H., He, X., Peeta, S., Zheng, T., Li, Y.: Evaluating the energy consumption of electric vehicles based on car-following model under non-lane discipline. Nonlinear Dyn. **82**(1), 1–13 (2015)
43. Anderson, G., Suner, C., Sardpour, A.: Visual information for car following by drivers: role of scene information. Transp. Res. Rec. J. Transp. Res. Board **1899**(1), 104–108 (2004)
44. Anderson, G., Sauer, C.: Optical information for car following: the driving by visual angle model. Hum. Factors **49**(5), 878–896 (2007)
45. Zhou, J.: An extended visual angle model for car-following theory. Nonlinear Dyn. **81**(1), 549–560 (2015)
46. Jin, S., Wang, D., Yang, X.: Non-lane-based car-following model with visual angle information. Transp. Res. Rec. J. Transp. Res. Board **2249**, 7–14 (2011)